

Scattering-Matrix Formulation for Both Measurement and Prediction of Acoustical Performances of Hybrid Cells and Their Active and Passive Elements

Azzedine Sitel¹⁾, Marie-Annick Galland²⁾

¹⁾ CSTB, Centre Scientifique et Technique du Bâtiment, 24 Rue Joseph Fourier, 38400 Saint Martin d'Hères, France. azzedine.sitel@free.fr

²⁾ Centre Acoustique du LMFA, Ecole Centrale de Lyon, 36 avenue Guy de Collongue, 69134, Ecully cedex, France

Summary

The design of panels improving both sound absorption and insulation performance over a wide frequency range is a problem of considerable practical interest for transport and building industries. In this work, an analytical method for predicting both the absorption coefficient and the transmission loss of hybrid active/passive multilayered cells and the associated experimental investigation are presented. These cells combine passive and active control by using passive layers and an active plate. Passive layers consist of absorbing materials located on the reception side in order to increase absorption over a wide frequency range. The active plate vibrates as a secondary source in order to reduce sound transmission at low and/or at resonance frequencies. To validate the analytical approach, measurement methods in ducts based on the scattering-matrix description are applied to characterise three types of system: (i)-passive discontinuities such as multilayered sandwiches including porous layers (ii)-active discontinuities here the active plate playing the secondary source role, (iii)-hybrid cells equipped with active control system. For these three cases, the correspondence between theoretical simulations and experimental results is satisfactory.

PACS no. 43.20.Gp, 43.20.Mv, 43.20.Ye, 43.40.At, 43.40.Dx, 43.40.Rj, 43.50.Gn

1. Introduction

Over the years, it has been shown that passive panels exhibit a lack of sound insulation at low frequencies, especially where structural resonances occur [1, 2]. Panels with only passive material require unacceptable quantities of absorbing materials to get high acoustic performances at low and resonance frequencies. Active control techniques using piezoelectric actuators can complement passive solutions at low and resonance frequencies while keeping a small weight and thickness. Indeed, to improve acoustic absorption for a wide frequency range, cells combining passive properties of absorbing materials and active control have been developed by Galland and all [3, 4]. The principle was therein based on the pressure cancellation realized behind porous material layer. The first major investigations on this hybrid concept were conducted by Guigou and Fuller [5] in order to reduce sound transmitted into an aircraft. In [6], Batifol *et al.* presented a finite-element model to predict insulation by

hybrid cells including poroelastic layers and piezoelectric patches. Recently, Chang and all [7] presented a theoretical model for predicting the sound absorption for a thin micro-perforated plate attached with piezoelectric patch and electrical circuits. This paper presents analytical and experimental methods based on the scattering-matrix description for predicting and measuring acoustical performances of active/passive sandwiches and their active and passive elements. Hybrid cells tested in this work combine active and passive approaches by using an active plate and passive layers. Passive layers include absorbing materials located at the reception side to increase absorption over a wide frequency range. The active plate acts as a secondary source of an active control system in order to reduce the sound transmission at low and resonance frequencies. It should be noted that hybrid cells tested here contain only one active control channel, the active feedback is optimized to minimize only the sound transmission. The absorption is passively assured at medium and high frequencies using porous layers. To optimize by active control both absorption and insulation at low frequencies, two active control channels would be necessary.

Received 3 December 2010,
accepted 17 March 2011.

In the case of passive multilayered panels, the analytical absorption coefficient α and the transmission loss TL can be deduced using transfer-matrix approach for the sandwich [8, 9]. A global matrix is easily deduced from the elementary transfer matrices associated with each element or interface of the passive sandwich under consideration.

In the case of hybrid cells (including sources), the transfer-matrix formulation is not suitable to model the problem due to active elements (noise control sources) in the hybrid sandwich. On the other hand, it has been shown by Abom [10, 11, 12, 13] that the scattering-matrix theory is better suited for predicting acoustical properties of both passive and active discontinuities in duct systems. This two-port matrix is used to predict and/or measure the performance of passive two-port discontinuities in ducts such as silencers or mufflers [11] as well as two-port sources [12] as for example: pumps, fans with one inlet and one outlet opening. Overall, the scattering-matrix formalism gives the best basic description of wave interaction problem (anechoic transmission and reflection on both sides of the discontinuity, symmetry...).

By analogy, the active plate which acts as a secondary source in hybrid cells is modelled here as a two-port source as described in section 2.2.

The simulation of the transmission loss and the absorption coefficient of hybrid cells in the case of active control is carried using the scattering-matrix formulation. In order to measure TL and α values of passive sandwiches in ducts, the majority of previous works use measurement methods such as the two-load method to determine the transfer-matrix [6, 13] or the measurement of transmission loss using anechoic terminations [14]... There are, however, some practical problems associated with these methods.

The two-load method has large errors sensitivity, especially, when element under test presents high transmission loss [13, 15]. The use of anechoic termination makes the measurement set-up large and quite expensive to build. In view of this, it seems appropriate that measurement methods for characterisation of passive and active two-port elements as well as the entire hybrid cells should be based on the scattering-matrix description.

In this work, characterisation inside a duct of passive discontinuities such as passive sandwiches or porous layers is carried out using the two source-location method [12]. This method is superior to the two-load method and has smaller error sensitivity [13]. Also, a measurement method used to determine two-port source data in form of a source strength vector and a scattering-matrix [12] is applied to characterize active and passive properties of the secondary source. Furthermore, unlike passive sandwiches, the scattering-matrix of hybrid cells in the case of active control, is not independent on the duct measurement conditions described in section 3.

Consequently, all previous measurement methods to determine the acoustical two-port matrices (described in [13]) are not valid when the two-port element under test is equipped with active control system. To overcome this

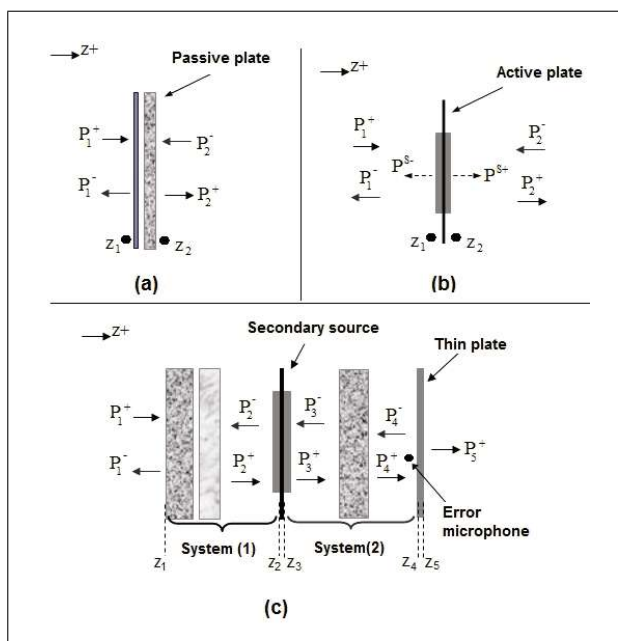


Figure 1. Schema of passive, active and hybrid two-port systems; (a) Passive sandwich excited on both sides by a plane wave; (b) Active plate excited on both sides by a plane wave; (c) General configuration of the studied hybrid cells.

difficulty, some suggestions are given in section 3.3 to adapt the two source-location method for measuring the scattering-matrix of hybrid cells for active control case.

In the first part of this paper, the scattering-matrix formulation describing the acoustical behaviour of passive panels and active plates is recalled. An analytical method is presented to predict, in the case of active control, both absorption coefficient and transmission loss of hybrid sandwiches including porous layers, air layers, elastic thin plate and an active plate. In the second part, the description of measurement procedures based on the scattering-matrix formulation is given for three cases: (i) passive layers or sandwiches, (ii) active plate, (iii) hybrid cells. In the third part, experimental and analytical results are presented and discussed. The elementary layers of the hybrid cells under study (elastic thin plate, poroelastic layer, and the secondary source) are considered first. Then, results of two different configurations of hybrid cells are discussed.

2. Theoretical basis and analytical simulation

2.1. Definition of the scattering matrix of passive systems

Consider a passive system (elastic plate or/and porous panels...) located between the axial coordinates z_1 on the left side and z_2 on the right side as shown in Figure 1a. Two plane waves are considered to excite this system on both sides. Under the assumption of linear theory, the acoustical behaviour of this panel can be described completely by its scattering-matrix $[S]_{2 \times 2}$ which implies a lin-

ear relationship between the incoming wave pressure vector $\{P_1^+(z_1), P_2^-(z_2)\}^T$ and the out coming wave pressure vector $\{P_1^-(z_1), P_2^+(z_2)\}^T$,

$$\begin{Bmatrix} P_1^-(z_1) \\ P_2^+(z_2) \end{Bmatrix}_2 = [S]_{2 \times 2} \begin{Bmatrix} P_1^+(z_1) \\ P_2^-(z_2) \end{Bmatrix}_2, \quad (1)$$

with $[S]_{2 \times 2} \begin{Bmatrix} S_{11} & S_{12} \\ S_{21} & S_{22} \end{Bmatrix}_{2 \times 2}$.

This matrix, which depends only on the panel and its boundary conditions, is independent of the upstream and the downstream acoustical conditions. The physical meaning of its 4 coefficients is as follows:

- S_{11} and S_{21} represent anechoic reflection and transmission coefficients, respectively, associated with the left side incoming wave.
- S_{22} and S_{12} represent anechoic reflection and transmission coefficients, respectively, associated with the right side incoming wave.

The anechoic absorption coefficient α and the transmission loss TL associated with the left side incoming waves can easily be deduced from scattering-matrix coefficients by

$$\alpha = 1 - |S_{11}|^2, \quad (2)$$

$$TL = 10 \log (1/|S_{21}|^2). \quad (3)$$

The acoustical behaviour of passive systems can also be described using the transfer-matrix $[Tr]_{2 \times 2}$ or the mobility-matrix $[Z]_{2 \times 2}$ descriptions [2, 8, 11]. The transfer-matrix method is usually used for modelling multilayered walls including passive layers without active elements [8, 9]. The scattering-matrix method is better suited for modelling two-port systems including active elements such as the active plate and/or hybrid cells presented in sections 2.2 and 2.3. Furthermore, the scattering matrix formalism uses the travelling wave amplitudes as state variables which have been shown to be more attractive than transfer or mobility matrices since it reflects the fundamental interaction waves allowing one to develop, for example, a general proposal for analyzing acoustic two-port networks [10]. However, the difference between $[Tr]_{2 \times 2}$, $[S]_{2 \times 2}$ and $[Z]_{2 \times 2}$ resides only in how the problem is depicted. So, when one type of these two-port matrices is known, the other matrix can be deduced from linear transformations [11, 15].

2.2. Definition of the acoustical data of the secondary source

Consider a vibrating thin elastic plate driven by two piezoelectric patches glued on each side of that plate as shown in Figure 1b. This active plate can be modelled as a two-port source [10, 12] having a radiated source vector $\{P^S\}_{2 \times 1}$ and a scattering-matrix $[S^S]_{2 \times 2}$. The relationship between the incoming pressure wave vector $\{P_1^+(z_1), P_2^-(z_2)\}^T$ and the out coming pressure wave vec-

tor $\{P_1^-(z_1), P_2^+(z_2)\}^T$ is written in this case

$$\begin{Bmatrix} P_1^-(z_1) \\ P_2^+(z_2) \end{Bmatrix}_2 = [S^S]_{2 \times 2} \begin{Bmatrix} P_1^+(z_1) \\ P_2^-(z_2) \end{Bmatrix}_2 + \{P^S\}_{2 \times 1} \quad (4)$$

with $[P^S]_{2 \times 1} = \begin{Bmatrix} P^{S-}(z_1) \\ P^{S+}(z_2) \end{Bmatrix}_2$.

P^{S+} and P^{S-} are the pressure radiated by the active plate on the right and the left side, respectively. The scattering-matrix $[S^S]_{2 \times 2}$ depicts the passive behaviour of the plate, while $\{P^S\}_{2 \times 1}$ represents its active behaviour. $\{P^S\}_{2 \times 1}$ and $[S^S]_{2 \times 2}$ are independent from the upstream and the downstream acoustical conditions.

2.3. Analytical simulation of acoustic absorption and insulation of hybrid cells

Hybrid sandwiches modelled in this work must be efficient in both absorption and acoustic insulation over a wide frequency range. A general combination to reach this goal is the sandwich given in Figure 1c. This combination consists of

- A system (1) located on the reception side in order to improve passively absorption. This system (1) can include absorbing elements such as poroelastic layers coupled with air cavities, and/or with microperforate plate...
- A rear sandwich composed of the active plate, the system (2) which can be an air cavity or air/porous/air and a thin plate located in the rear face. The active plate vibrates as a secondary source in order to reduce the pressure level at the error microphone position located at z_4 . The goal of this sandwich (active plate/system(2)/thin plate) is to improve by active control the global sound insulation of the entire cell.

Calculations of absorption coefficient and transmission loss of this hybrid cell are deduced from equations (5)–(9) described below:

- The scattering-matrix $[S^S]_{2 \times 2}$ of the system (1) located between axial coordinates z_1 and z_2 leads to relationships between $\{P_1^+(z_1), P_2^-(z_2)\}^T$ and $\{P_1^-(z_1), P_2^+(z_2)\}^T$:

$$\begin{Bmatrix} P_1^-(z_1) \\ P_2^+(z_2) \end{Bmatrix}_2 = [S^1]_{2 \times 2} \begin{Bmatrix} P_1^+(z_1) \\ P_2^-(z_2) \end{Bmatrix}_2. \quad (5)$$

- The acoustical source data of the active plate in form of its scattering-matrix $[S^S]_{2 \times 2}$ and its source radiated vector $\{P^{S-}(z_2), P^{S+}(z_3)\}^T$ gives the following equations system:

$$\begin{Bmatrix} P_2^-(z_2) \\ P_3^+(z_3) \end{Bmatrix}_2 = [S^S]_{2 \times 2} \begin{Bmatrix} P_2^+(z_2) \\ P_3^-(z_3) \end{Bmatrix}_2 + \begin{Bmatrix} P^{S-}(z_2) \\ P^{S+}(z_3) \end{Bmatrix}_2. \quad (6)$$

- The scattering-matrix $[S^S]_{2 \times 2}$ of the system (2) located between z_3 and z_4 leads to

$$\begin{Bmatrix} P_3^-(z_3) \\ P_4^+(z_4) \end{Bmatrix}_2 = [S^2]_{2 \times 2} \begin{Bmatrix} P_3^+(z_3) \\ P_4^-(z_4) \end{Bmatrix}_2. \quad (7)$$

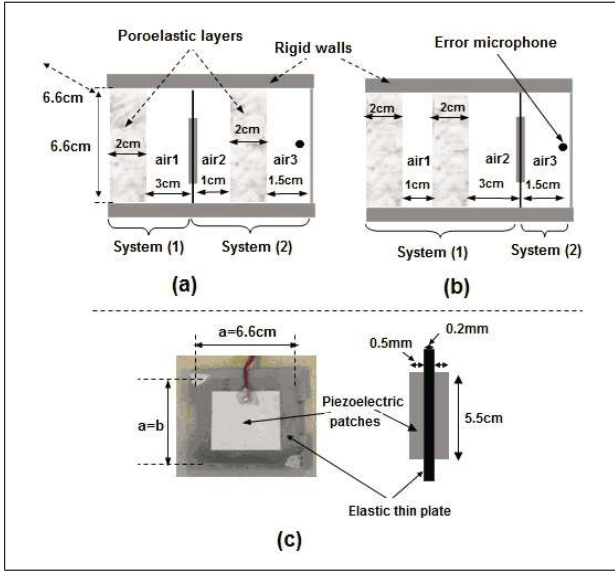


Figure 2. Schema and dimensions of the two tested hybrid cells and of the used active plate; (a) Cell (A): porous/air1/active plate/air2/porous/air3/elastic thin plate; (b) Cell (B): porous/air1/porous/air2/active plate/air3/elastic plate; (c) Photo and dimensions of the active plate.

- In the case of anechoic upstream acoustic conditions ($P_5^-(z_5) = 0$), the scattering-matrix $[S^{PI}]_{2 \times 2}$ of the elastic thin plate located between z_4 and z_5 gives

$$\begin{Bmatrix} P_4^-(z_4) \\ P_5^+(z_5) \end{Bmatrix}_2 = [S^{PI}]_{2 \times 2} \begin{Bmatrix} P_4^+(z_4) \\ 0 \end{Bmatrix}_2. \quad (8)$$

- The used active plate is symmetrical with respect to its right and left sides since the two piezoelectric patches glued on its two sides are identical (see Figure 2c). Radiated pressures P^{S-} and P^{S+} can therefore be related by the following relationship:

$$P^{S-}(z_2) = -P^{S+}(z_3). \quad (9)$$

From equations (5)–(9), we can calculate $P_4(z_4)$ as well as the reflected and transmitted pressures $P_1^-(z_1)$ and $P_5^+(z_5)$ on the reception and the transmission side, respectively:

$$P_4(z_4) = g_1 P_1^+(z_1) + g_2 P^{S+}(z_3), \quad (10)$$

$$P_1^-(z_1) = g_3 P_1^+(z_1) + g_4 P^{S+}(z_3), \quad (11)$$

$$P_5^+(z_5) = g_5 P_1^+(z_1) + g_6 P^{S+}(z_3). \quad (12)$$

Parameters $g_{i=1..6}$ are as a function of scattering-matrix coefficients of $[S^1]_{2 \times 2}$, $[S^2]_{2 \times 2}$, $[S^{PI}]_{2 \times 2}$ and $[S^S]_{2 \times 2}$ computed by combining equations (5)–(9). Those scattering-matrices are deduced from analytical transfer-matrices $[Tr^1]_{2 \times 2}$, $[Tr^2]_{2 \times 2}$, $[Tr^{PI}]_{2 \times 2}$ and $[Tr^S]_{2 \times 2}$ associated respectively, to the systems (1), (2), the elastic thin plate and the active plate. The radiated pressure allowing the cancellation of the sound pressure level $P_4(z_4)$ at the error sensor position is deduced from equation (10),

$$P^{S+}(z_3) = -(g_1/g_2)P_1^+(z_1). \quad (13)$$

Table I. Physical properties and dimensions of structures composing cells (A) and (B) depicted in Figure 2.

Lateral dimensions of all elements	
Width	$a = 6.6 \text{ cm}$
Length	$b = 6.6 \text{ cm}$
Elastic steel thin plate	
Thickness	$h = 0.2 \text{ mm}$
Mass density	$\rho_S = 7700 \text{ kg/m}^3$
Young's modulus	$E = 2 \cdot 10^{11}(1 - 0.01j)$
Poisson's ratio	$\nu = 0.33$
Active plate	
Mean thickness	$h = 0.33 \text{ mm}$
Mean mass density	$\rho_S = 15000 \text{ kg/m}^3$
Mean Young's modulus	$E = 2 \cdot 10^{11}(1 - 0.1j)$
Poisson's ratio	$\nu = 0.33$
Poroelastic layers (foam)	
Thickness	$e_1 = e_2 = 2 \text{ cm}$
Flow resistivity	$\sigma = 26 \text{ Rayls/m}$
Porosity	$\phi = 0.95$
Tortuosity	$\alpha_\infty = 1.1$
Viscous characteristic dimension	$\Lambda = 150 \mu\text{m}$
Thermal characteristic dimension	$\Lambda' = 220 \mu\text{m}$
Poisson's ratio of the skeleton	$\nu = 0.3$
Young's modulus of the skeleton	$E = 1 \cdot 10^5(1 + 0.1j)$
Solid mass density	$\rho = 100 \text{ kg/m}^3$
Air cavities	
Fluid mass density	$\rho_0 = 1.213 \text{ kg/m}^3$
Sound speed	$c_0 = 342 \text{ m/s}$

We can introduce in equation (13) a factor χ to describe the active control intensity as

$$P^{S+}(z_3) = -\chi(g_1/g_2)P_1^+(z_1). \quad (14)$$

$\chi = 1$ means that the pressure at z_4 is equal to zero (active control fully working); $\chi = 0$ means that there is only passive control, active control being off. If for example $\chi = 0.8$, active control reduces 80% of the sound pressure level at the control point.

Reflection and transmission coefficients at z_1 and z_5 , respectively, are determined from (11), (12) and (14):

$$R(\chi) = P_1^-(z_1)/P_1^+(z_1) = (g_3 - \chi(g_1 g_4/g_2)), \quad (15)$$

$$T(\chi) = P_5^+(z_5)/P_1^+(z_1) = (g_5 - \chi(g_1 g_6/g_2)). \quad (16)$$

Absorption coefficient $\alpha(\chi)$ and transmission loss $TL(\chi)$ of the hybrid cells presented in Figure 1c can finally be deduced from equations (2), (15), (3) and (16).

Two hybrid combinations (A) and (B) are tested in this paper (Figures 2a and 2b). For the cell (A), the system (1) consists of a porous layer coupled with air cavity (porous/air), while the system (2) is air/porous/air. Their associated transfer-matrices are equal to:

$$[Tr^1]_{2 \times 2} = [Tr^{por(1)}]_{2 \times 2} \cdot [Tr^{air(1)}]_{2 \times 2}, \quad (17)$$

$$[Tr^2]_{2 \times 2} = [Tr^{air(1)}]_{2 \times 2} \cdot [Tr^{por(2)}]_{2 \times 2} \cdot [Tr^{air(3)}]_{2 \times 2}. \quad (18)$$

For (B), the system (1) is porous/air/porous/air, while the system (2) is a simple air cavity, so

$$[Tr^1]_{2 \times 2} = [Tr^{por(1)}]_{2 \times 2} \cdot [Tr^{air(1)}]_{2 \times 2} \cdot [Tr^{por(2)}]_{2 \times 2} \cdot [Tr^{air(2)}]_{2 \times 2}, \quad (19)$$

$$[Tr^2]_{2 \times 2} = [Tr^{air(3)}]_{2 \times 2}. \quad (20)$$

$[Tr^{air(1,2,3)}]_{2 \times 2}$ is the transfer-matrix of air layers in the case of a plane wave excitation [2]. $[Tr^{por(1,2,3)}]_{2 \times 2}$ is the transfer-matrix of the used poroelastic layers analytically calculated by Biot-Allard model [2]. The elastic thin plate is modelled here as a simply supported plate with infinite lateral dimensions. To consider finite dimensions ($a = b = 6 \text{ cm}$) its transfer-matrix $[Tr^{Pl}]_{2 \times 2}$ is deduced from its impedance adjusted in order to account the first flexural mode [16]. Due to the geometry of the active plate (Figure 2c), its transfer-matrix $[Tr^S]_{2 \times 2}$ is deduced by the same way considering equivalent parameters (thickness, mass density and Young's modulus) determined by adjusting analytical curves to experimental ones. Of course, those analytical matrices do not correspond exactly to practical conditions, but, they can be used for testing the hybrid cells simulation approach presented here. Indeed, the cells elements have small lateral dimensions ($a = b = 6.6 \text{ cm}$) and are coupled only with air layers. Therefore, effects of some parameters such as higher vibration modes of elastic thin plates and finite lateral dimensions of porous layers are neglected. Alternatively, when analytic calculations are too complicated (complexes boundary conditions, active plate with several piezoelectric patches...), all those matrices can be deduced by numerical [17, 18, 19] and/or experimental methods presented below in section 3 and then introduced in the numerical implementation of the analytical theory described above.

3. Measurement methods

The characterization of passive sandwiches, the active plate and hybrid cells is based on the measurement of the scattering-matrix $[S]_{2 \times 2}$. Experiments were carried out by a rectangular duct including segments made with 0.5 cm thick steel walls which have 6.6 cm internal width and length. Figure 3a shows the following elements:

- A test segment for fixing a sample under test.
- Two identical sources (1) and (2) fixed on each ends of this duct.
- Two measurement sections to separate travelling waves P^+ and P^- in both sides of the test segment.

During all measurements, sources (1) and (2) were driven with a white noise signal in the frequency band [20–2000 Hz]. For those frequencies, the acoustic excitation inside the measurement duct is a plane wave with normal incidence. The determination of the scattering-matrix of passive, active and hybrid systems has been carried out using the two source-location method [13] which is based on the measurement of positive and negative travelling waves P^\pm

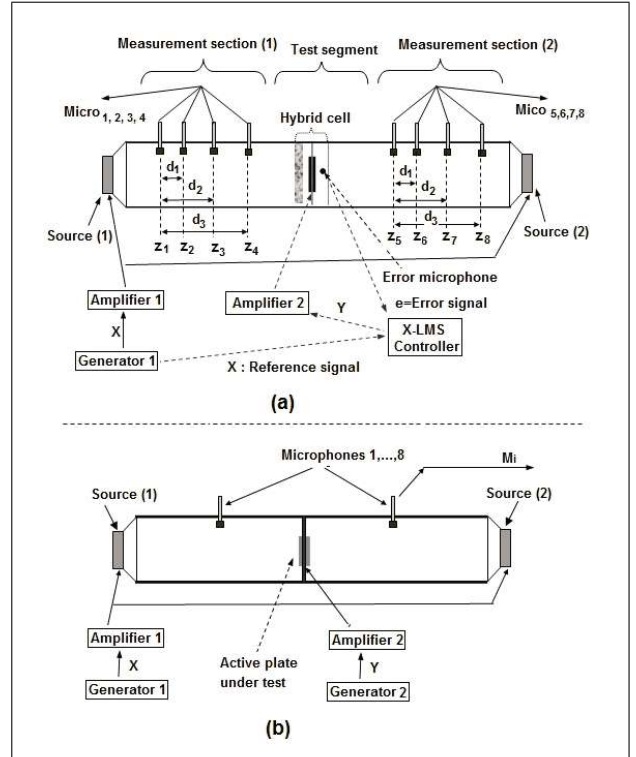


Figure 3. Experimental duct used to measure the scattering-matrix of two-port discontinuities; (a) Experimental setup for the characterization of passive elements and/or hybrid cells; (b) Experimental setup for the characterization of the active plate.

in both sides of the test segment for two different acoustical duct conditions. These two different conditions are obtained using the two source-location method [13]. The first one was obtained by switching on the source (1), while the source (2) was switched off leading to

$$\begin{Bmatrix} P_1^-(z_4)^I \\ P_2^+(z_5)^I \end{Bmatrix}_2 = [S^I]_{2 \times 2} \begin{Bmatrix} P_1^+(z_4)^I \\ P_2^-(z_5)^I \end{Bmatrix}_2. \quad (21)$$

The second condition was obtained by switching on the source (2), while the source (1) was switched off,

$$\begin{Bmatrix} P_1^-(z_4)^{II} \\ P_2^+(z_5)^{II} \end{Bmatrix}_2 = [S^{II}]_{2 \times 2} \begin{Bmatrix} P_1^+(z_4)^{II} \\ P_2^-(z_5)^{II} \end{Bmatrix}_2. \quad (22)$$

$P_1^\pm(z_4)$ and $P_2^\pm(z_5)$ depict pressure waves travelling in the positive and negative z directions in measurement sections 1 and 2 at z_4 and z_5 , respectively. Superscripts (I) and (II) indicate the two different acoustic conditions of the measurement duct. Four microphones M_i were used to separate P^\pm positive and negative travelling waves on each side of the sample under test. The two-microphone method is known to give poor results when the wavelength λ is closed to twice the distance between the microphones [20]. An overdetermination technique [15] using a number of equations higher than the number of unknowns allows avoiding this problem. $P_1^\pm(z_4)$ and $P_2^\pm(z_5)$ were de-

terminated as

$$\begin{Bmatrix} P_1^+(z_4) \\ P_1^-(z_4) \end{Bmatrix}_{2 \times 1} = \left[\left[[D^+]_{2 \times 4} \cdot [D^+]_{2 \times 4}^T \right]^{-1} * [D^+]_{2 \times 4} \right]_{2 \times 4} \{P_1\}_{4 \times 1}, \quad (23)$$

$$\begin{Bmatrix} P_2^+(z_5) \\ P_2^-(z_5) \end{Bmatrix}_{2 \times 1} = \left[\left[[D^-]_{2 \times 4} \cdot [D^-]_{2 \times 4}^T \right]^{-1} * [D^-]_{2 \times 4} \right]_{2 \times 4} \{P_2\}_{4 \times 1}, \quad (24)$$

where $[D^+]_{2 \times 4}$ and $[D^-]_{2 \times 4}$ are 2×4 matrices used for separation in sides (1) and (2).

$$[D^\pm]_{2 \times 4}^T = \begin{bmatrix} 1 & e^{\pm jkd_1} & e^{\pm jkd_2} & e^{\pm jkd_3} \\ 1 & e^{\mp jkd_1} & e^{\mp jkd_2} & e^{\mp jkd_3} \end{bmatrix}. \quad (25)$$

$d_1 = 5$ cm, $d_2 = 15$ cm, $d_3 = 45$ cm, are distances between the microphone 1 and 2, 1 and 3, 1 and 4, respectively. $\{P_1\}_{4 \times 1}^T = \{P(z_{i=1,2,3,4})\}_{4 \times 1}^T$ and $\{P_2\}_{4 \times 1}^T = \{P(z_{i=5,6,7,8})\}_{4 \times 1}^T$ are the pressure vectors on the two sides. $P(z_i)$ is the acoustic pressure at z_i deduced from the transfer function $H_{M_i, X}$ between the microphone signal M_i and the reference signal X . The calibration of microphones has been carried out using the transfer function method [21] avoiding the use of calibration sources.

3.1. Characterization of passive systems

When the element under test is passive or when the active control system is turned off, the scattering-matrix is independent on acoustical conditions inside the measurement duct, so

$$[S]_{2 \times 2} = [S^I]_{2 \times 2} = [S^{II}]_{2 \times 2}. \quad (26)$$

$[S]_{2 \times 2}$ is determined from equations (21) and (22) as

$$[S]_{2 \times 2} = [P^{out}]_{2 \times 2} \cdot [P^{in}]_{2 \times 2}^{-1}. \quad (27)$$

$[P^{in}]_{2 \times 2}^{-1}$ and $[P^{out}]_{2 \times 2}^{-1}$ are input and output waves matrices whose two columns are associated to two measurement duct conditions (I) and (II) described by equations (21) and (22),

$$[P^{in}]_{2 \times 2} = \begin{bmatrix} P_1^{+(I)}(z_4) & P_1^{+(II)}(z_4) \\ P_2^{-(I)}(z_5) & P_2^{-(II)}(z_5) \end{bmatrix}, \quad (28)$$

$$[P^{out}]_{2 \times 2} = \begin{bmatrix} P_1^{-(I)}(z_4) & P_1^{-(II)}(z_4) \\ P_2^{+(I)}(z_5) & P_2^{+(II)}(z_5) \end{bmatrix}. \quad (29)$$

The signal driving sources (1) or (2) is taken here as the reference signal. It should be noted that the determination of the matrix $[S]_{2 \times 2}$ can also be carried out using the two-source method where the two measurement conditions (I) or (II) are obtained by switching on simultaneously the sources (1) and (2). To have an invertible matrix $[P^{in}]_{2 \times 2}$, properties of one-port sources (1) and (2) associated to

measurement condition (I) must be different from those associated to measurement condition (II).

The two source-location method used in this work has a smaller error sensitivity than the two-source or the two-load methods and enables to better avoid singular frequencies for solving equation (27) [13].

3.2. Characterisation of the radiating plate

In order to determine the active plate performances, its scattering-matrix $[S^S]_{2 \times 2}$ and its source strength vector $\{P^S\}_{2 \times 1}$ have to be determined. The measurement procedure consists in two steps:

- Firstly, $[S^S]_{2 \times 2}$ was determined using the method described above for the passive case.
- Secondly, using eq. (4), the radiated vector $\{P^{S-}(z_4), P^{S+}(z_5)\}^T$ was determined from the measured scattering-matrix $[S^S]_{2 \times 2}$ and from pressure vectors $\{P_1^+(z_4), P_2^-(z_5)\}^T$ and $\{P_1^-(z_4), P_2^+(z_5)\}^T$ measured by turning off the external sources (1) and (2),

$$\begin{Bmatrix} P^{S-}(z_4) \\ P^{S+}(z_5) \end{Bmatrix}_2 = \begin{Bmatrix} P_1^-(z_4) \\ P_2^+(z_5) \end{Bmatrix}_2 - [S^S]_{2 \times 2} \begin{Bmatrix} P_1^+(z_4) \\ P_2^-(z_5) \end{Bmatrix}_2. \quad (30)$$

In this step, $\{P_1^+(z_4), P_2^-(z_5)\}^T$ and $\{P_1^-(z_4), P_2^+(z_5)\}^T$ have been deduced from the measured transfer functions $H_{M_i, Y}$ where the electrical signal Y driving the active plate is taken as the reference signal (see Figure 3b).

3.3. Characterisation of hybrid cells performances

Active control is realised using the filtered-X LMS algorithm [3, 4, 5, 6]. Unlike passive sandwiches, the scattering-matrix of hybrid cells depends on upstream and downstream acoustical conditions inside the measurement duct when the active control is turned on. So, $[S^I]_{2 \times 2}$ associated with the first measurement condition (I) is not equal to $[S^{II}]_{2 \times 2}$ associated to the measurement condition (II) ($[S^I]_{2 \times 2} \neq [S^{II}]_{2 \times 2}$). Consequently, all previous measurement methods [13] developed to determine acoustical two-port matrices are not valid in this case. In order to adapt the two source-location method to active control case, the scattering-matrix $[S^{II}]_{2 \times 2}$ associated to the measurement condition (II) must be identical to $[S^I]_{2 \times 2}$ associated to the measurement condition (I). To get such condition (II), the sound level and the phase of the source (2) must be adjusted so that the error microphone indicates a value e_{II} equal to e_I for both modulus and phase and for each frequency (see Figure 3a). Note that e_I and e_{II} are the error microphone signals (before turning on the active control) associated with measurement conditions (I) and (II) as described by equations (21) and (22). By this way, the scattering-matrix of two-port hybrid systems can be deduced from equation (27). The experimental absorption coefficient α and transmission loss TL in the case of active control are finally deduced from the measured matrix $[S]_{2 \times 2}$ via equations (2) and (3).

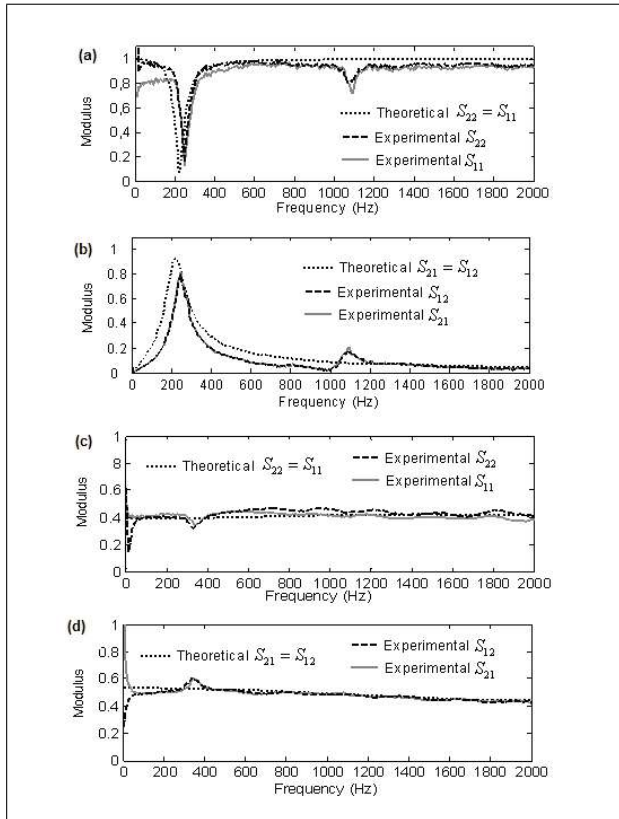


Figure 4. Comparison between experimental and analytical modulus of scattering-matrix coefficients of passive elements composing the studied hybrid cells; (a) Reflection coefficients S_{11} and S_{22} of a rectangular simply supported elastic thin plate; (b) Transmission coefficients S_{21} and S_{12} ; (c) Reflection coefficients S_{11} and S_{22} of a rectangular poroelastic layer; (d) Transmission coefficients S_{21} and S_{12} .

4. Presentation and analysis of results

Experimental curves are plotted versus frequency up to 2000 Hz for a normal incidence plane wave excitation. Physical properties and dimensions of elements composing the tested cells (porous layer, elastic plate, active plate) are listed in Table I. Poroelastic parameters of the porous material used by the analytical model [2] have been determined by the characterization techniques given in [22].

4.1. Results of elements composing the studied hybrid cells

Figures 4a and 4b represent experimental and analytical modulus of the scattering-matrix coefficients, S_{11} , S_{22} , S_{12} and S_{21} of a simply supported elastic thin plate used in the tested hybrid cells. The agreement between analytical and experimental curves is generally very good. Four comments have to be made:

1. Peaks and dips are noted on anechoic transmission $\{S_{12}, S_{21}\}$ and reflection $\{S_{22}, S_{11}\}$ coefficients. The first (at 250 Hz) and secondary (at 1100 Hz) peaks and dips are due to the resonance of the first and the second flexural modes of the plate, respectively.

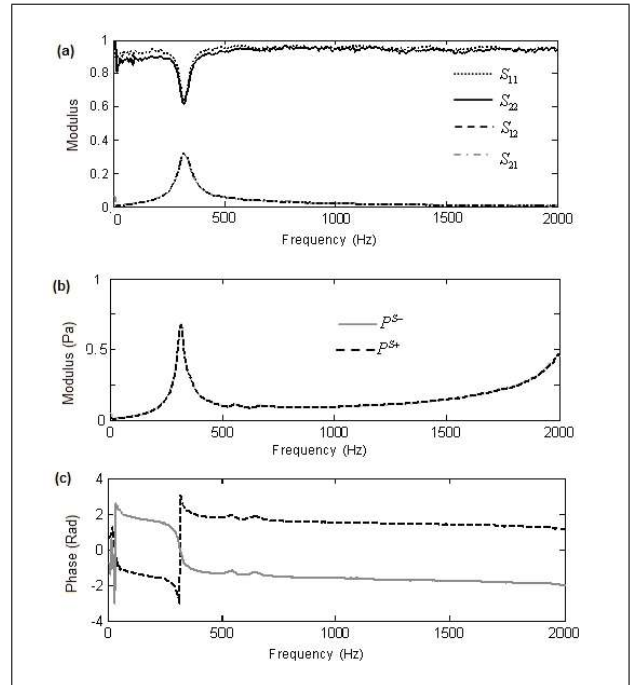


Figure 5. Experimental scattering-matrix $[S]_{2 \times 2}$ and radiated pressures $P^{S\pm}$ of the active plate. (a) Modulus of S_{11} , S_{22} , S_{12} and S_{21} ; (b) Modulus of $P^{S\pm}$; (c) Phase of $P^{S\pm}$.

2. Peaks and dips of experimental curves are slightly shifted to low frequencies with respect to analytical curves. This is due to experimental mounting conditions of the plate which is not perfectly simply supported.
3. The absence of the second mode (at 1100 Hz) on analytical curves is related to the used analytical model which takes into account only the first flexural mode.
4. For frequencies higher than 200 Hz, curves of anechoic reflection coefficients S_{11} and S_{22} associated to incoming waves from the left and the right side, respectively are nearly super-imposed, verifying then the symmetry of the plate. For low frequencies below 200 Hz, the symmetry is not verified ($S_{22} \neq S_{11}$). This is due to poor performances at very low frequencies of the used external sources (1) and (2) (see Figure 12).

Figure 4c shows experimental and analytical modulus of anechoic reflection coefficients $\{S_{11}, S_{22}\}$ for a rectangular poroelastic layer (inserted in the experimental duct), Figure 4d shows the modulus of its anechoic transmission coefficients $\{S_{12}, S_{21}\}$. The agreement between the calculated and measured coefficients is good. A small difference between coefficients S_{11} and S_{22} is however observed for frequencies higher than 800 Hz showing that the porous layer is not totally symmetrical. This can be explained by a small difference between both faces of the porous layer. Also, a ‘small dip’ on experimental curves of $\{S_{21}, S_{12}\}$ and a ‘small peak’ on curves of $\{S_{11}, S_{22}\}$ are clearly noticeable around 360 Hz. This is due to the resonance of the first flexural mode of the poroelastic rectangular layer. As expected, resonances are not seen in analytical curves because calculation was carried out with infinite lateral dimensions.

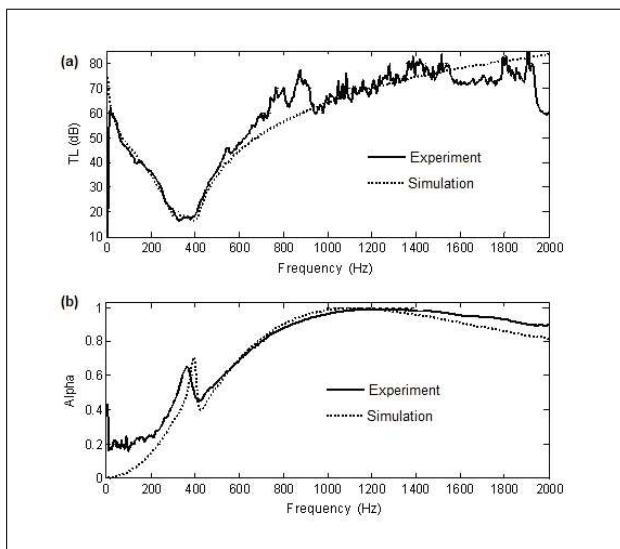


Figure 6. Experimental and analytical performances of hybrid cell (A) for passive case; (a) Transmission loss TL (dB); (b) Absorption coefficient α .

Figure 5a shows experimental modulus of the active plate scattering-matrix coefficients. The active plate under test is simply supported and shown in Figure 2c. Curves of experimental scattering-matrix coefficients point out a symmetrical passive behaviour since $S_{22} = S_{11}$. Effects of the added mass due to the piezoelectric patches are obvious: the resonance magnitude (around 320 Hz) of the active plate flexural mode is less important than that of the simple plate without patches (Figures 4a and 4b).

Figure 5b shows the experimental modulus of pressures radiated by the active plate on the right and the left side P^{S+} and P^{S-} , respectively. Those radiated pressures are measured by the method described in section 3.2. The modulus of P^{S+} and P^{S-} is important in particular around the first and the second modes of the active plate whose the resonance frequency is closed to 400 Hz and 2000 Hz. Far from those two frequencies, the modulus of P^{S+} and P^{S-} is relatively low. On the other hand, P^{S+} and P^{S-} are nearly superimposed (Figure 5b), and their phases are π shifted (Figure 5c) verifying the symmetry of the active behaviour of the plate. Consequently, the use of equation (9) to account the symmetry of the secondary source is validated.

4.2. Results of hybrid cells

In Figures 6a and 6b, the analytical and experimental curves of absorption coefficient and transmission loss TL of the sandwich (A) are compared without active control case. Mostly, the agreement between theory and experiment is very good. For the frequency range [500–2000 Hz], experiment and theory show satisfactory performances of the sandwich (A) on both absorption and acoustic insulation ($\alpha > 0.6$, $TL > 40$ dB). A discrepancy between experiment and theory is however noted below 150 Hz. This difference is due to the low level of pressures radiated by sources (1) and (2) at very low frequencies

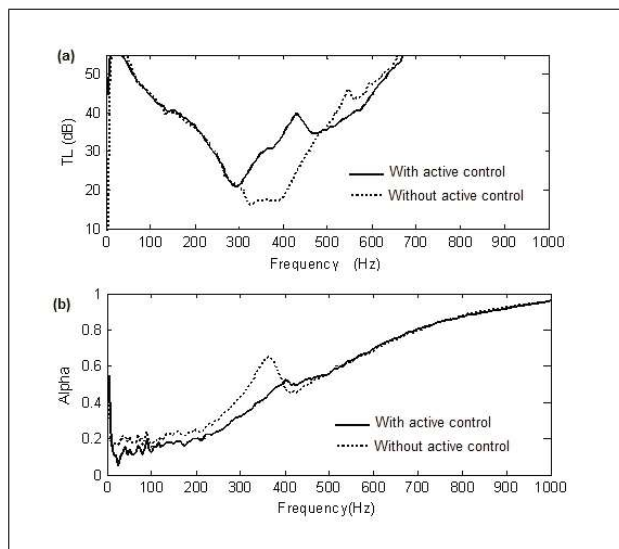


Figure 7. Experimental performances of hybrid cell (A) with and without active control; (a) Transmission loss TL (dB); (b) Absorption coefficient α .

(see Figure 12). This makes the determinant of the matrix $[P^{in}]_{2 \times 2}$ (defined by equation 28) closed to zero [13] and then increases error sensitivity of the method used to measure the scattering-matrix.

Figures 7a and 7b show experimental results of TL and α of cell (A) with and without active control. Using active control, a significant gain (more than 15 dB) has been obtained in transmission loss around resonances (between 350 and 500 Hz). For those frequencies the experimental absorption coefficient α decreases when the active control is applied. This is due to the pressure $P^{S-}(z_4)$ radiated by the active plate towards the reception side having here a negative effect in terms of absorption. Far-off resonances, the difference between passive and active control curves is insignificant.

To improve absorption without increasing thickness and mass, the sandwich (B) (Figure 2b) is selected from prediction results and then experimentally tested. Without active control (Figure 8), both theory and experiment show its higher absorbing performance than sandwich (A). Indeed, for frequencies higher than 400 Hz, the coefficient is higher than 0.8 and for frequencies located between 250 and 400 Hz, α is between 0.5 and 0.8. In terms of acoustic insulation (Figure 8a), the sandwich (B) is inferior to (A). In fact, in the case of cell (B), the system (2) is a simple air cavity with a small thickness ($z_4 - z_3 = 1$ cm). So, the active plate mode resonance is quite far from the mass-spring-mass resonance of the system (active plate/ system (2) /elastic plate). Consequently, the transmission loss of (B) is much reduced for a larger frequency range located between two dips (around 400 Hz and 550 Hz) compared with cell (A) (one dip).

In the case of active control (Figure 9), there are two remarks:

- The active control is efficient only around the frequency resonance of the active plate located 400Hz. The second

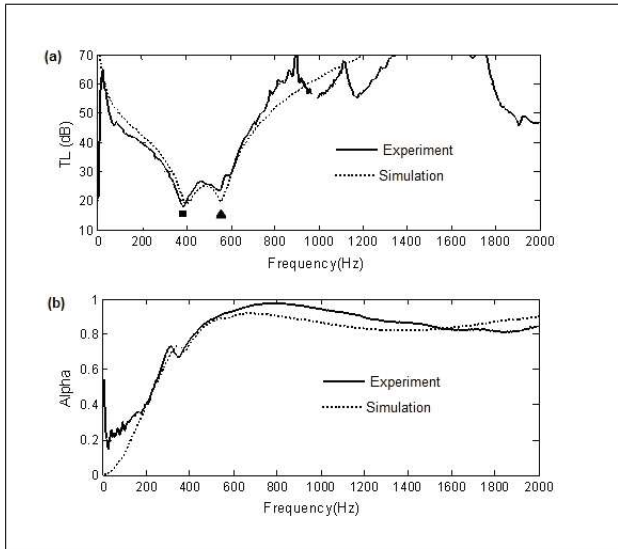


Figure 8. Experimental and analytical performances of hybrid cell (B) for passive case; (a) Transmission loss TL (dB); (b) Absorption coefficient α ; The symbols ■ and ▲ denote the active plate mode resonance and the mass-spring-mass resonance of cell (B).

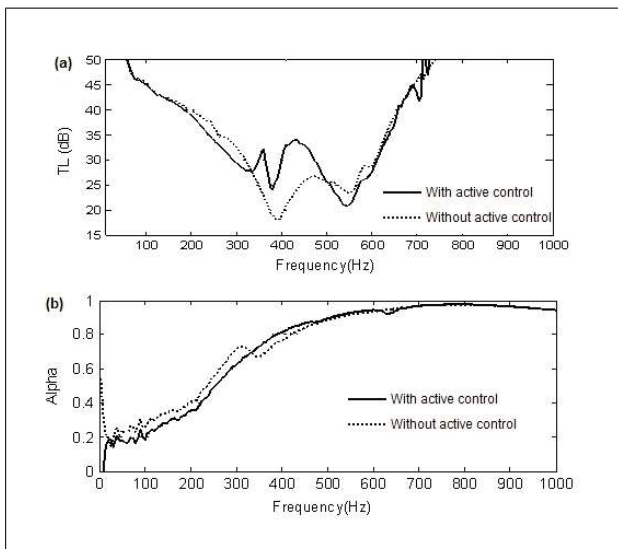


Figure 9. Experimental performances of hybrid cell (B) with and without active control; (a) Transmission loss TL (dB); (b) Absorption coefficient α .

dip of the transmission loss located near of 550Hz has not been significantly reduced by active control. This is due to the low level of the frequency response $P^{S^+}(f)$ of the used secondary source near of 550 Hz. We can conclude that as a secondary source of an active control system, the used active plate is efficient only around the frequency resonance of its flexural modes.

- By using two porous layers in the reception side, negative effects (on absorption) of radiated pressure $P^{S^-}(z_4)$ towards the reception side is negligible.

Figure 10 depicts analytical α and TL of the sandwich (A) in the case of active control. Those analytical curves are deduced from equations (15) and (16) with different ac-

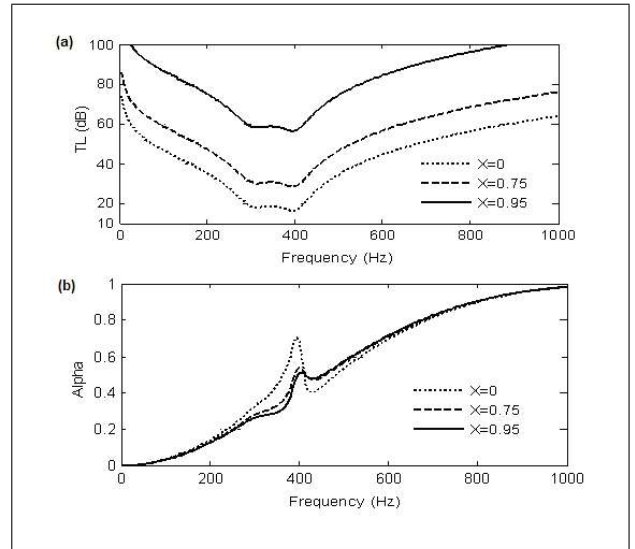


Figure 10. Predicted acoustical performances of cell (A). (a) Transmission loss TL (dB); (b) Absorption coefficient α .

tive control intensities according to the factor χ ($\chi = 0, 0.75, 0.95$). Around resonances (near 400 Hz), analytical absorption coefficient agrees with experiment (Figure 7b) since α diminishes due to $P^{S^-}(z_4)$ effects when the active control is applied ($\chi = 0.75, 0.95$). With active control, a gain on TL (10 dB for and 40 dB for $\chi = 0.95$) is obtained in the whole studied frequency range. Nevertheless, experiment has shown that active control is efficient only near of the active plate mode frequency (around of 400Hz). This difference is of course normal since the active plate frequency response is considered invariant in the prediction by taking the factor χ invariant versus the frequency. To account for the actual frequency response, the factor χ used in equations (15) and (16) is replaced by $\chi'(f)$ including the normalised radiated pressure $P^{S^+}(f)$ as follows:

$$\chi'(f) = \chi |P^{S^+}(f)|. \quad (31)$$

Figure 11 represents transmission loss of sandwiches (A) and (B) simulated using the measured radiated pressure P^{S^+} in equation (31) for $\chi = 0; 0.75$. At once, the agreement between experiment (Figures 7a and 9a) and simulation (Figures 11a and 11b) is now excellent. For both sandwiches (A) and (B), the transmission loss has been improved by active control, but only around the first resonance frequency of the active plate. To get a high acoustic insulation in the whole frequency range, the system (2) of the general configuration of hybrid cells presented in Figure 1c must be chosen so that the mass-spring-mass frequency resonance of the whole cell should be closed to the frequency resonance of the active plate. On the other hand, for thicknesses L lower than 10 cm, all combinations of hybrid cells presented in Figure 1c can not allow good absorption at very low frequencies ($f < 300$ Hz). It is however possible to improve absorption performances for middle and high frequencies by using a system (1) configuration in the reception side similar to the sandwich (B)

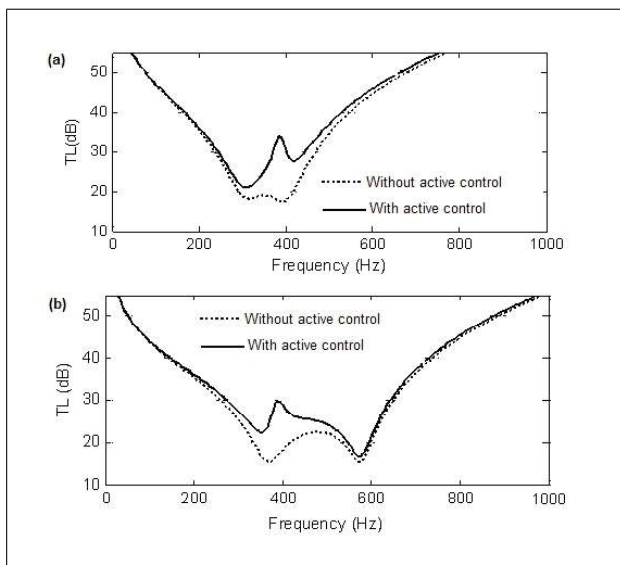


Figure 11. Transmission loss of cells (A) and (B) simulated (with and without active control) taking into account the experimental frequency response of the secondary source.

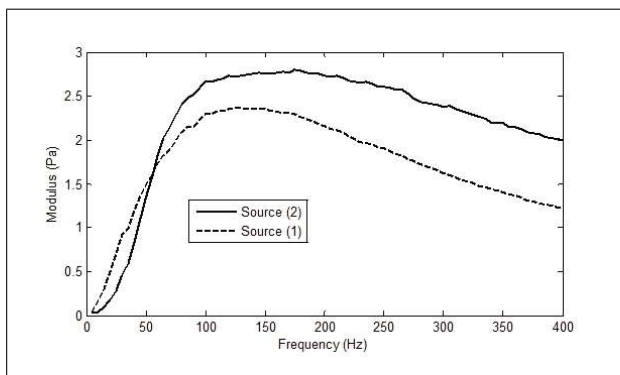


Figure 12. Spectrums of radiated pressures of one-port sources (2) and (1) used to measure the scattering-matrix.

one. To greatly improve the absorption coefficient and the transmission loss at very low frequencies while keeping a small thickness, two active control channels would be necessary.

5. Conclusion

Analytical and experimental methods based in the scattering-matrix formulation have been applied to model and to measure the transmission loss and the absorption coefficient of hybrid cells as well as acoustical performances of their active and passive elements. The studied hybrid cells use active control for reducing the sound transmission at low and resonance frequencies and passive control for improving the sound absorption at medium and high frequencies. A good agreement has been found between theory and experiment for two different hybrid configurations and for their active and passive elements. This confirms the simulation approach efficiency presented in this

work as well as a good precision of the used experimental methods. This work has shown that:

- The characterisation of the secondary source in form of a vector of radiated pressures and a scattering-matrix gives a best complete description of secondary sources properties allowing a good prediction or/and optimisation of hybrid cells acoustical performances.
- The use of an active plate vibrating as a secondary source through piezo-electric patches allows good active control performances, but only close to its resonance frequency. Around this frequency, a significant gain on transmission loss (higher than 15 dB) has been obtained by active control.
- An appropriate choice of the system (porous layers + air cavities) located in the reception side allows good absorption performance for a wide frequency band between 200 and 2000 Hz.

In spite of its simplicity, the proposed simulation approach is an efficient tool for modelling or optimizing multilayered hybrids cells. Indeed, when cells elements cannot be modelled by analytical methods (ex: complex element geometries, boundary conditions, ...), numerical or experimental data in form of scattering-coefficients or radiated-pressures can easily be incorporated in numerical implementations of the described formulations. This enables to easily model complex hybrid cells configurations with a smaller computation time compared with numerical methods modelling the whole structure at the same time.

In future works, hybrid cells with two active control channels will be tested in order to increase simultaneously absorption and acoustic insulation at low frequencies. Effects of oblique incidence and diffuse field will also be investigated.

Acknowledgement

The authors thank the support of the project PARABAS (Parois Acoustiques Basses Fréquences: ANR-06-BLAN-0081-01).

References

- [1] C. Lesueur: Rayonnement acoustique des structures. Eyrolles, Paris, 1988.
- [2] J. F. Allard: Propagation of sound in porous media: Modelling sound absorbing materials. Elsevier, New York, 1993.
- [3] M. A. Galland, B. Mazeaud, N. Sallen: Hybrid passive/ active absorbers for flow duct. *Applied Acoustics* **66** (2005) 691–708.
- [4] M. Furstoss, D. Thenail, M.-A. Galland: Surface impedance control for sound absorption: direct and hybrid passive/ active strategies. *J. Sound. Vib.* **203** (1997) 219–236.
- [5] C. Guigou, C. R. Fuller: Control of aircraft interior broadband noise with foam-pvdf smart skin. *J. Sound. Vib.* **220** (1999) 541–557.
- [6] C. Batifol, T. G. Zielinski, M. N. Ichchou, M.-A. Galland: A finite-element study of a piezoelectric/poro-elastic sound package concept. *Smart Mater. Struct.* **16** (2007) 168–177.

- [7] D. Chang, B. Liu, X. Li: An electromechanical low frequency panel sound absorber. *J. Acoust. Soc. Am.* **128** (2010) 639–645.
- [8] M. L. Munjal: Response of a multi-layered infinite plate on an oblique plane wave by means of transfer matrices. *J. Sound. Vib.* **162** (1993) 333–343.
- [9] B. Brouard, D. Lafarge, J. F. Allard: A general method of modelling sound propagation in layered media. *J. Sound. Vib.* **183** (1995) 129–142.
- [10] R. Glav, M. Abom: A general formalism for analyzing acoustic 2-port networks. *J. Sound. Vib.* **202** (1997) 739–747.
- [11] M. Abom: Measurement of the scattering matrix of acoustical two-ports. *Mech. Syst. Sig Proc.* **5** (1991) 89–104.
- [12] J. Lavrenjev, H. Bodèn, M. Abom: A measurement method for determination the source data of acoustic two-port sources. *J. Sound. Vib.* **197** (1996) 1–16.
- [13] M. Abom: A note on the experimental determination of acoustical two-port matrices. *J. Sound. Vib.* **155** (1992) 185–188.
- [14] J. D. Sagers, T. W. Leishman, J. D. Blotter: Active sound transmission control of a double-panel module using decoupled analog feedback control: experimental results. *J. Acoust. Soc. Am.* **128** (2010) 2807–2816.
- [15] A. Sitel, J. M. Ville, F. Foucart: Multiload procedure for measurement of acoustic scattering-matrix of a duct discontinuity for higher order modes propagation conditions. *J. Acoust. Soc. Am.* **120** (2006) 2478–2490.
- [16] T. Dupont: Transparence et absorption acoustiques des structures microperforées. PhD thesis, Institut National des Sciences Appliquées de Lyon, 2002.
- [17] A. Sitel, M.-A. Galland, C. Guigou-Carter: Modélisation numérique et caractérisation expérimentale des cellules hybrides efficaces en isolation acoustique sur une large bande de fréquences. 10th French Congress on Acoustics, April 2010.
- [18] N. Atalla, R. Panneton, P. Debergue: A mixed displacement-pressure formulation for poro-elastic materials. *J. Acoust. Soc. Am.* **104** (1444-1452) 1998.
- [19] R. Panneton, N. Atalla: Numerical prediction of sound transmission through finite multilayered systems with poro-elastic materials. *J. Acoust. Soc. Am.* **100** (1996) 346–354.
- [20] H. Boden, M. Abom: Influence of errors on the two-microphone method for measuring acoustic properties in ducts. *J. Acoust. Soc. Am.* **79** (1985) 541–549.
- [21] J. Y. Chung, D. A. Blaser: Transfer function method of measuring in-duct acoustic properties: I. Theory, II. Experiment. *J. Acoust. Soc. Am.* **63** (1980) 907–921.
- [22] N. Sellen, M.-A. Galland, O. Hilbrunner: Identification of the characteristic parameters of porous media using active control. AIAA/CEAS Aeroacoustics conference, Breckenridge, Colorado, USA, 17-19 June 2002.